

## CHAPTER 4

### INFRARED SPECTROSCOPIC STUDY OF PHASE TRANSFORMATIONS IN LIQUID CRYSTALLINE CBOOA

#### 4.1 Introduction

In the previous chapter on the far-infrared and the Raman spectra of crystalline CBOOA, the occurrence of a solid-solid transition below the onset of the smectic A phase was demonstrated and the implications of this transition for the formation of the mesophase were considered. The purpose of this chapter is to present and discuss the results of a near and far-infrared study of liquid crystalline CBOOA in its different phases. The experimental results are discussed in relation to the influence of molecular structure on the far-infrared absorption of the fluid phases as well as certain features characterizing the crystal-smectic A transition.

#### 4.2 Experimental

Near infrared spectra were recorded in the range 2-15  $\mu$  using the Leitz double beam prism spectrograph. Samples were contained between a pair of NaCl windows. Solid samples in Phase I were prepared without using any

spacer between the windows. The resultant polycrystalline film, a few microns thick, was adequate to yield good, reproducible spectra. The liquid crystal and isotropic phases were studied using samples of 20  $\mu$  thickness, a mylar spacer being used for this purpose. Nematic liquid crystalline samples aligned in the homeotropic configuration were prepared following the method described in Chapter 2. These samples showed good extinction under crossed polarizers. Also upon cooling to the smectic A phase, the homeotropic alignment was still very well preserved.

Far infrared spectra in the range 30-700  $\text{cm}^{-1}$  were obtained using the Polytec FIR-30 Fourier spectrometer. The range 30-700  $\text{cm}^{-1}$  was covered using spectral range Nos. 1, 2 and 3 (see table 2.1, Chapter 2). Sample cells with a-quartz windows were employed in the region 30-250  $\text{cm}^{-1}$ , while diamond windows were used in the range 250-700  $\text{cm}^{-1}$ . The spectral resolution was between 3-4  $\text{cm}^{-1}$ . The spectrum of Phase II (of the solid) was investigated using a thin layer of sieved powder. Polycrystalline samples of Phase I were obtained by slow cooling and solidification of a bubble free film of the liquid crystal.

For dichroic measurements in the range 30-250  $\text{cm}^{-1}$ , homogeneously aligned liquid crystalline samples were

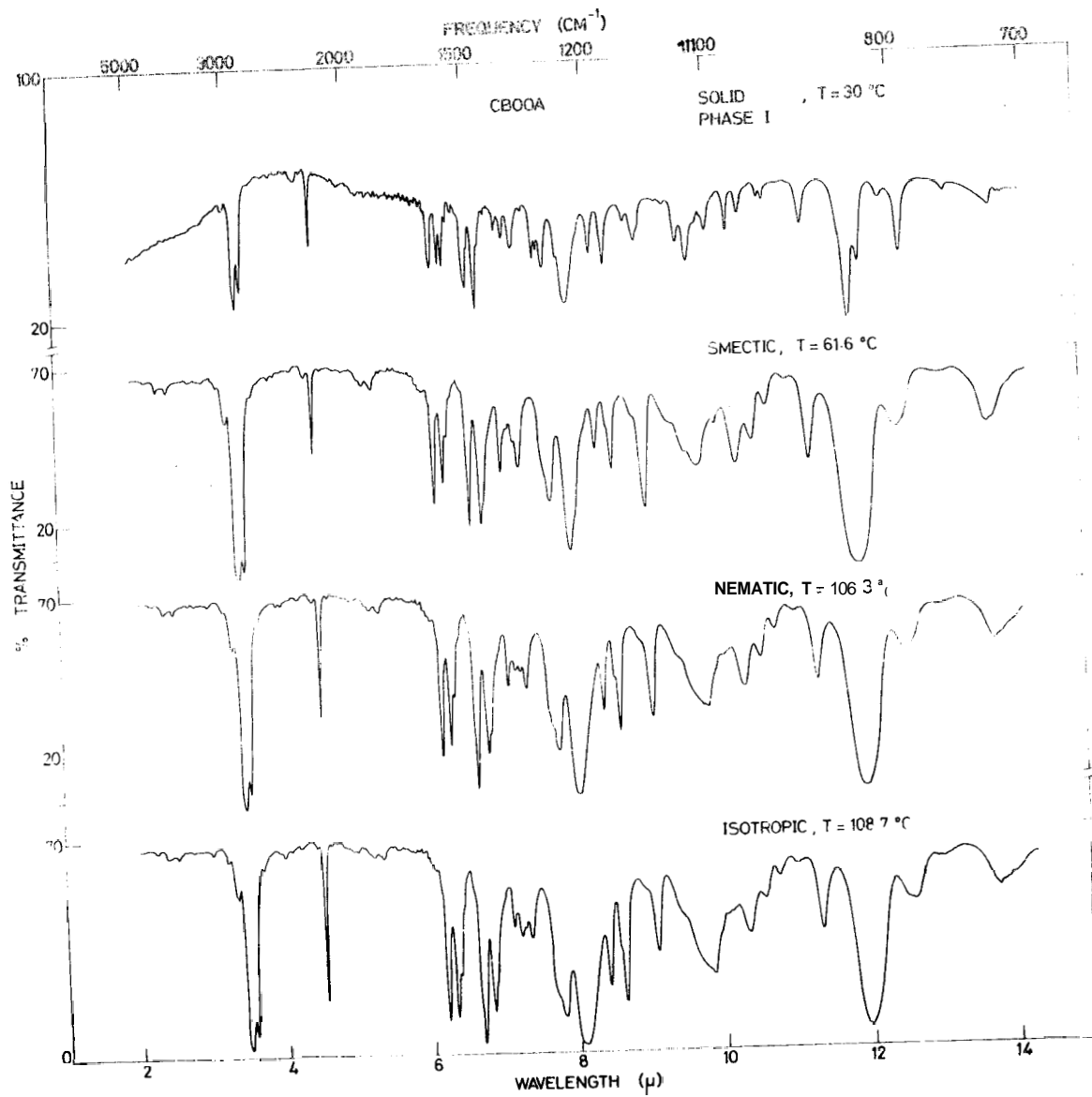
contained between square a-quartz windows and the experiments were carried out as described in chapter 2.

#### 4.3. Experimental Results and Discussion

(a) Near Infrared spectra: Figure 4.1 shows the near infrared spectra of the different phases of CBOOA, in the range 2-15  $\mu$ . Spectra of solid Phase XI are not shown because except for minor intensity changes, no significant differences were observed as compared to the spectra of Phase I. As noted in Chapter 3, in the internal mode region, the Raman spectra of the two phases also show a similar behaviour. This is consistent with the expectation that when the crystal symmetry of a complex molecular crystal changes due to a polymorphic transition, the intramolecular modes would be affected much less compared to the intermolecular modes. From Fig. 4.2 we note that in a few cases, the characteristic splittings observed in the solid (Phase I) disappear in the fluid phases. The spectra of smectic A and nematic phases were obtained using homeotropically aligned samples. The flat baseline at wavelengths shorter than 3  $\mu$  indicates that the alignment is very good. If we define the 'dichroic ratio' R as the ratio of the integrated absorption of the band in the Liquid crystal to that in the isotropic, we see, on comparing the intensities of the bands in the fluid phases that R is less than unity for certain bands, while it is greater than unity for some others. (This is indicative of the fact that the transition dipole moments

**FIGURE 4.1**

**Near infrared spectra of CBOOA in the solid (Phase I), smectic A, nematic and isotropic phases. The temperature corresponding to each phase is also shown.**



of these bands have their major component along the long axis or perpendicular to the long axis of the molecule, respectively. The observed 'dichroic' ratio of each band is hence useful in ascertaining the predominant polarization direction of that band. Along with the observed frequencies of the bands, the polarization features of the bands are also useful in making vibrational assignments to the spectra. To consider some examples, the strong modes at  $\sim 970$  and  $838 \text{ cm}^{-1}$  are assigned to out-of-plane C-H vibrations of the benzene rings and all of these do have  $R > 1$ . In contrast, the mode at  $1160 \text{ cm}^{-1}$  which is assigned to a skeletal mode of the octyl tail ( $\omega_c$ ) may be expected to have  $R < 1$  and this is what is observed. The  $-\text{C}\equiv\text{N}$  stretching mode at  $2247 \text{ cm}^{-1}$  provides another clear illustration of this type of behaviour, the transition moment being nearly parallel to the long axis of the molecule.

The vibrational assignments to the Raman and far-infrared spectra of the solid phases of CBOOA were given in Chapter 3. As noted there, there is some overlap between the frequency regions of the various possible modes arising from the different molecular units constituting CBOOA. In addition, designations such as rocking and twisting modes are only approximate as considerable coupling between these motions can occur in a complex molecule. For these reasons, complications can arise in

the assignments of some of the modes. However, from a comparison of the present spectra with those of other liquid crystals<sup>1-3</sup> and organic compounds that contain structural groups similar to those comprising CBOOA, a tentative correlation of several of the observed modes with characteristic group vibrations can be made. The observed infrared frequencies together with the assignments proposed on this basis are listed in Table 4.1. The frequencies below  $650 \text{ cm}^{-1}$  were obtained from the far-infrared measurements which are discussed below.

#### (b) Far Infrared Spectra

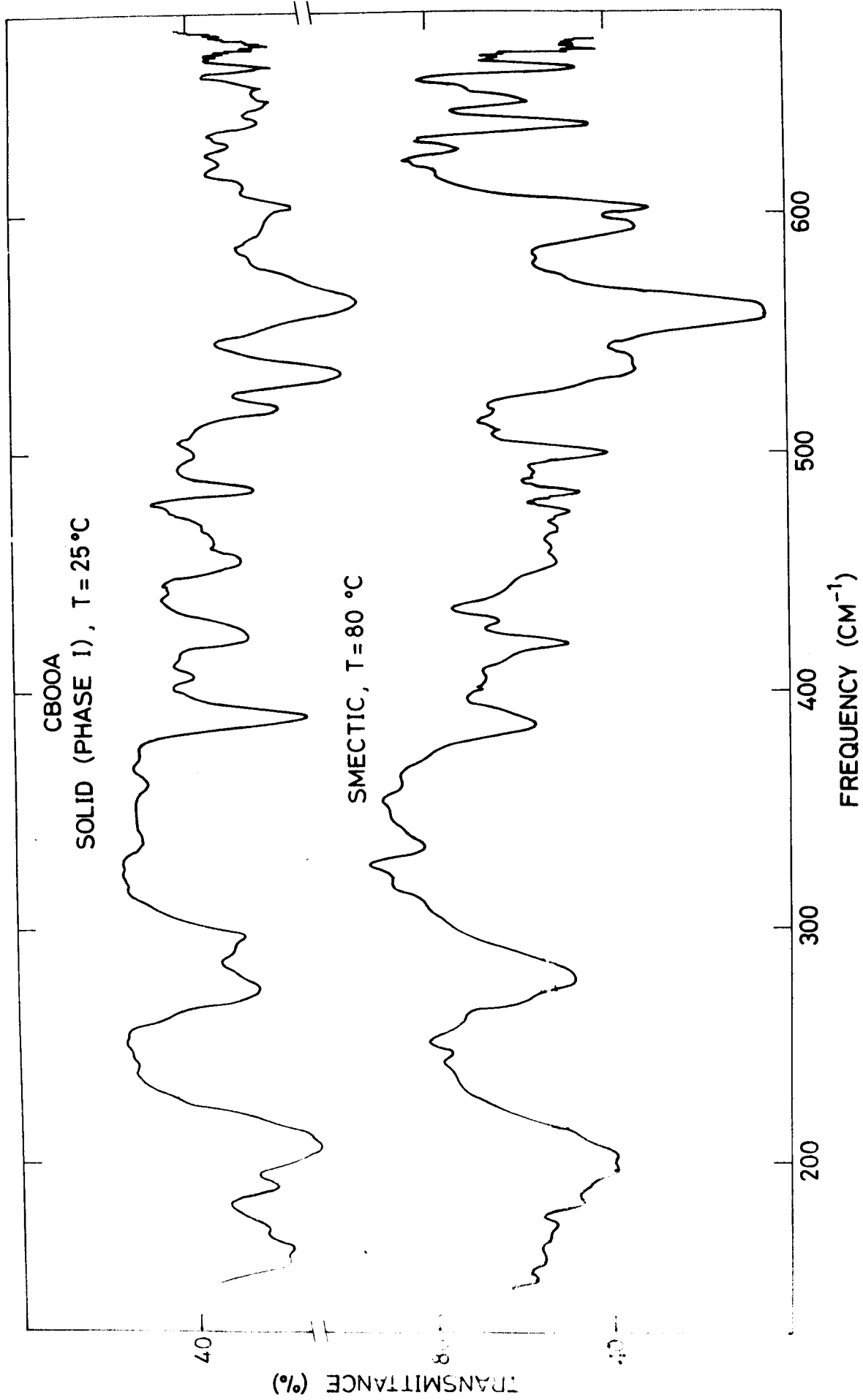
(I) Crystal-Mesophase Transition: The far-infrared spectra of the solid (Phase I) and smectic A phases, in the range  $150\text{-}650 \text{ cm}^{-1}$ , are shown in Fig. 4.2. Spectra of the nematic and isotropic phases were almost identical to that of the smectic A phase and hence they are not shown here. Owing to an upper limit of  $\sim 40 \mu$  on the average particle size in samples of Phase 31, strong scattering was present in the range above  $300 \text{ cm}^{-1}$  and this made it difficult to obtain meaningful spectra of Phase II at higher frequencies.

While some intensity differences are apparent between the two spectra shown in Figure 4.2, the observed frequencies in the solid and smectic A phase are almost identical except for two interesting features, which we

**FIGURE 4.2**

**Far-infrared absorption spectra of CBOOA in the solid (Phase I) and smectic A phases. The temperature corresponding to each phase is also indicated.**



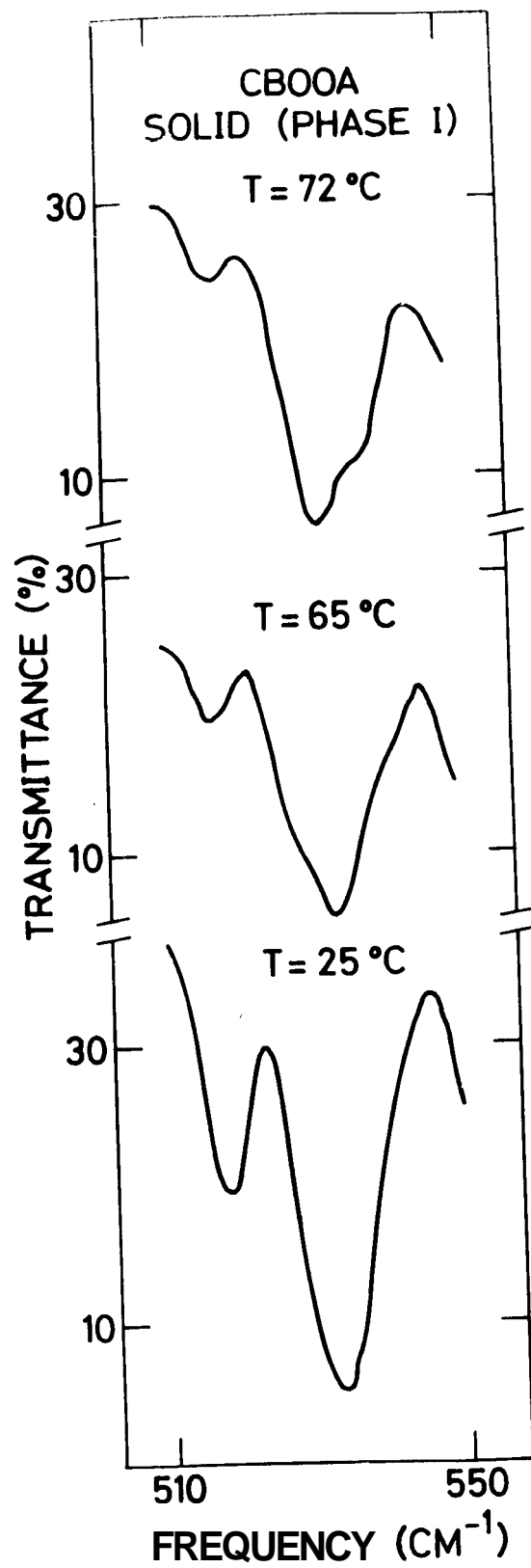


consider below in further detail. First, the distinct mode observed in the crystal at  $518\text{ cm}^{-1}$  is absent in the smectic A phase. We have followed the intensity change of this mode in relation to the neighbouring line at  $530\text{ cm}^{-1}$ , as a function of temperature, and this is shown in Fig. 4.3. The mode at  $530\text{ cm}^{-1}$  undergoes some broadening and attenuation in intensity as the temperature approaches the crystal-smectic A transition and such a behaviour was noticeable in the cases of other neighbouring lines also. However, the mode at  $518\text{ cm}^{-1}$  is seen to exhibit a much more rapid change in intensity in comparison to the line at  $530\text{ cm}^{-1}$ . The former nearly disappears at the crystal-smectic A transition, whereas the mode at  $530\text{ cm}^{-1}$  persists in the smectic A phase, although with reduced intensity. From an infrared study of *p*-azoxyanisole and its higher homologues, Bulkin et al. reported a similar behaviour;<sup>4</sup> the intensity of certain mid-infrared bands was found to decrease continuously as the crystal-nematic transition was approached from below. However, they noted that this phenomenon could not be observed near a crystal-smectic transition. The present results show that such effects can occur near the crystal-smectic transition also.

In all these cases, the disappearing infrared bands occur at too high a frequency to correspond to typical lattice modes. Bulkin et al. suggested<sup>4</sup> that such bands

**FIGURE 4.3**

Temperature dependence of the far-  
infrared absorption of polycrystalline  
CBOOA (Phase I), in the range  $500\text{-}550\text{ cm}^{-1}$ .



could be combination modes between external and internal vibrations and related the disappearance of the bands to the onset of progressive disorder in the lattice. In the case of crystal-nematic transition, the pretransition effects observed in the infrared spectra were attributed to the movement of molecules from lattice to interstitial sites,<sup>4</sup> leading to positional disorder in the lattice. More recently, Kirov and Simova<sup>5</sup> have also adopted the same reasoning. However, neutron scattering studies by Riste et al.<sup>6</sup> indicate that the pretransition effects in the vicinity of the crystal-nematic transition are caused by increasing rotational freedom of the molecules rather than positional disorder. During a study of p-azoxyanisole these authors noticed that with increasing temperature, the integrated intensity of several Bragg diffracted peaks decreased gradually and became zero at the crystal-nematic transition. Also, two broad, diffuse peaks characteristic of the nematic phase were seen to emerge in the crystalline phase itself nearly 10°C below the transition to the mesophase and their intensity was seen to increase as the transition point was approached from below. The widths of the disappearing Bragg peaks were found to be essentially independent of temperature. This implies that long range correlations of molecular centres of mass are maintained until the onset of the liquid crystalline phase and that these pretransition changes are not effected by positional

disorder. On the basis of model calculations,<sup>7</sup> Riste et al. have concluded that the changes observed by them can be accounted for by assuming that the molecules execute uncorrelated, torsional oscillations about their long axes, the amplitude of the oscillations increasing as the temperature is raised towards the crystal-nematic transition. The molecules, however, were assumed to remain parallel and at the sites of a rigid lattice till the melting point was reached. This picture thus corresponds to progressive rotational disorder rather than positional disorder; it also suggests that the positional order is lost in such systems in a much more abrupt manner very close to the melting point. The latter notion is not inconsistent with the theory of melting presented by Kobayashi<sup>8</sup> for liquid crystalline materials. As emphasized by Kobayashi, the apparently gradual disappearance of the translational order parameter at the melting point, as seen from his calculations, is a consequence of certain simplifying assumptions and it is not essential to the theory.

The above model of rotational disorder may also be applicable to crystal-smectic transitions involving the less ordered smectic phases; in these cases also, as at the crystal-nematic transition, the molecules become nearly free to rotate about their long axes at the transition temperature.

As the external vibrations of a crystal would be sensitive to changes in lattice forces and intermolecular coupling, one might expect that their behaviour in the pretransition region would provide a direct check of either hypothesis. For-infrared<sup>3, 9-12</sup> and Raman spectra<sup>2, 13-16</sup> of low-frequency modes have been reported for materials exhibiting crystal-nematic transition. In all these cases, the pretransition effects generally consist of broadening and intensity changes in the spectra. It should however be mentioned that the interpretation of the results as reported in these cases does not permit one to unambiguously conclude as to whether rotational or positional disorder is the dominant cause of these changes.

More definitive results have been reported in the low-frequency modes of mesogens exhibiting crystal-smectic transitions. The crystal structure of smectogenic compounds is known to exhibit a parallel, layered arrangement of molecules with some interpenetration between adjacent layers.<sup>17, 18</sup> This is to be contrasted with the imbricated structure found in nematogenic materials. At the crystal-smectic transition, the coupling between the layers is weakened and the spacing between them increases, thus allowing them to glide freely, one on top of the other. An intermolecular mode arising from the coupling of molecules in adjacent layers is then expected to reflect these changes preceding the melting of the crystal. On

this basis, Amer and Shen<sup>19</sup> as well as Dvorjetski et al.<sup>20</sup> have interpreted the softening of low-frequency Raman modes near the crystal-smectic transition as arising from a pre-melting relaxation of the bonding between layers. The latter authors also note that this process is probably accompanied by increased rotational motion of the molecules around their long axes.

From the foregoing considerations, the intensity variation of the band at  $518\text{ cm}^{-1}$  in Fig. 4.3 can be explained qualitatively if it is attributed to a combination between a 'soft', low-frequency intermolecular mode and an internal vibration. The direct observation of the low-frequency mode in question has not yet been reported in this case. From earlier studies,<sup>19,20</sup> it seems likely that this mode can occur at a frequency below  $30\text{ cm}^{-1}$ , a range not covered in our study of the vibrational spectra of CBOOA. The softening of the intermolecular mode probably occurs due to the increased rotational freedom of the molecules accompanied by the weakening of inter-layer coupling, while approaching the crystal-smectic transition. The relative contribution of these two factors can be assessed only after crystal structural and neutron scattering data on CBOOA become available over a sufficient temperature interval preceding the crystal-smectic transition.

The role played by conformational changes in alkyl

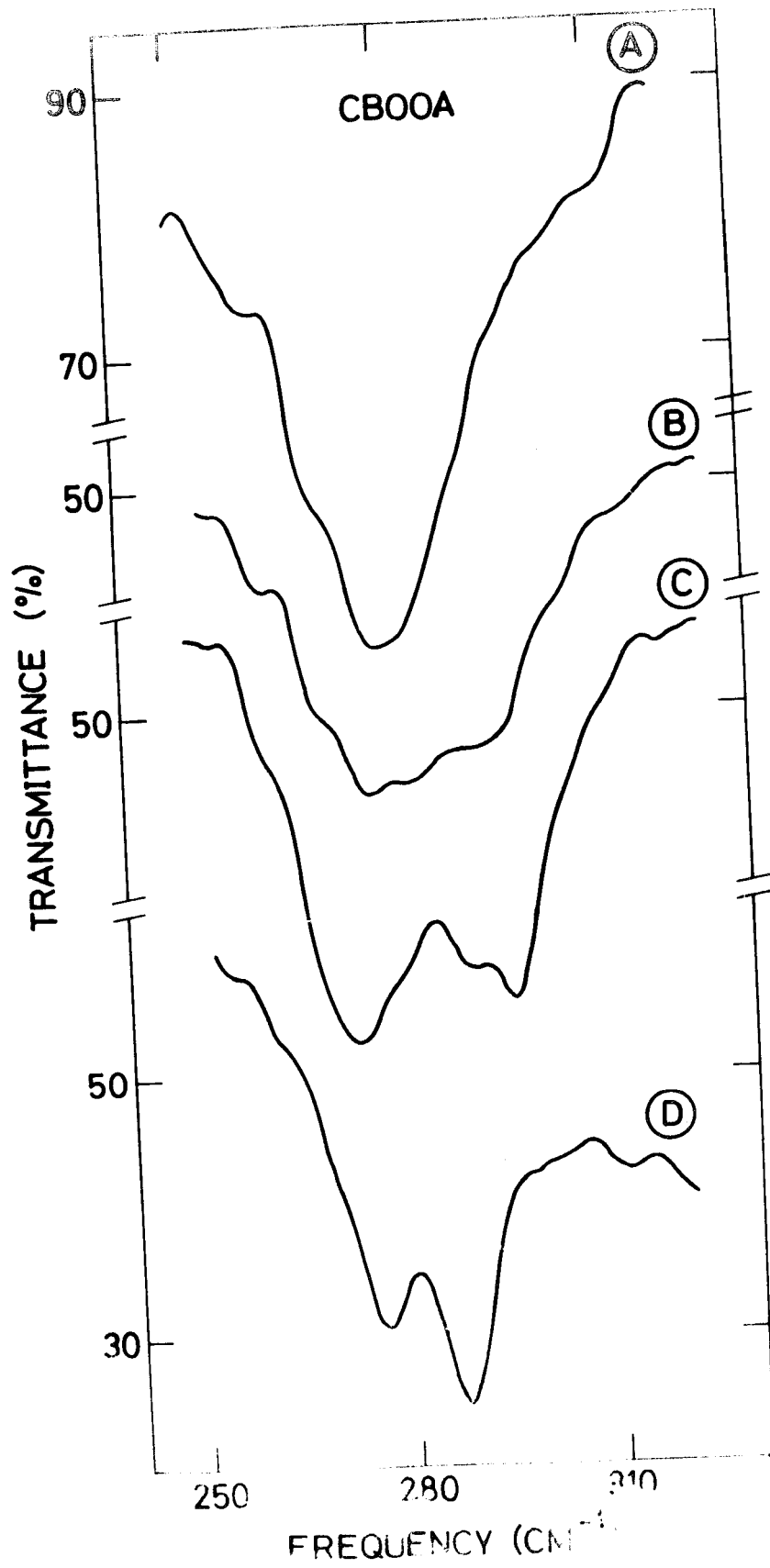


chains is also of considerable interest in the study of solid-fluid phase transitions. In the case of n-alkanes, the polymethylene chain is known to adopt the Sully extended, trans conformation in the solid phase, while many possible gauche conformers resulting in chain shortened forms appear in the fluid phases. Schaufele<sup>21</sup> obtained evidence for such a behaviour from a study of the longitudinal, accordion like modes associated with the chain backbone. Also, Schnur<sup>22</sup> found a similar behaviour during a Raman study of alkoxyazoxybenzene series of liquid crystals. As compared to the solid phase, the intensity of the bands assigned to the accordion mode was seen to decrease markedly upon entering mesophase. This was interpreted to signify that the allowed conformations of the alkoxy tails differ significantly between the various phases. As the CBOOA molecule possesses a long octyl tail, we expect on the basis of previous results<sup>21,22</sup> that a similar accordion mode may be observable in the present case also; if so, it should occur in the frequency range between 250-300  $\text{cm}^{-1}$ . Considering the molecular symmetry of CBOOA, the mode can exhibit infrared activity.

Figure 4.4 shows the detailed behaviour of the different phases in this range, as a function of temperature. Bath Phase II and Phase I are seen to exhibit two absorption maxima at room temperature. The band at the higher frequency occurs at 288  $\text{cm}^{-1}$  in Phase II and at 296  $\text{cm}^{-1}$

#### FIGURE 4.4

Far-infrared absorption spectra of the solid and smectic A phases of CBOOA in the range  $250\text{--}330\text{ cm}^{-1}$ . (A) Smectic A ( $80^\circ\text{C}$ ); (B) Solid (Phase I) ( $72^\circ\text{C}$ ); (C) Solid (Phase I) ( $25^\circ\text{C}$ ); (D) solid (Phase II) ( $25^\circ\text{C}$ ).



in Phase I. The slight shift in the position of this band is probably related to the differences in the molecular environment and crystal structure between the two solid phases. At temperatures above 65°C, the doublet is still clearly present in the solid (Phase I), although some broadening is evident. At the transition to the smectic A phase, the mode at 296  $\text{cm}^{-1}$  virtually disappears, as was the case in the nematic and isotropic phases. This behaviour is in agreement with that already observed in alkoxyazoxybenzenes<sup>22</sup> and hence the mode at 296  $\text{cm}^{-1}$  is identified as the 'accordion' mode belonging to the octyl tail. This value is also in good agreement with the calculated value<sup>23</sup> of 300  $\text{cm}^{-1}$  for the case of n-octane.

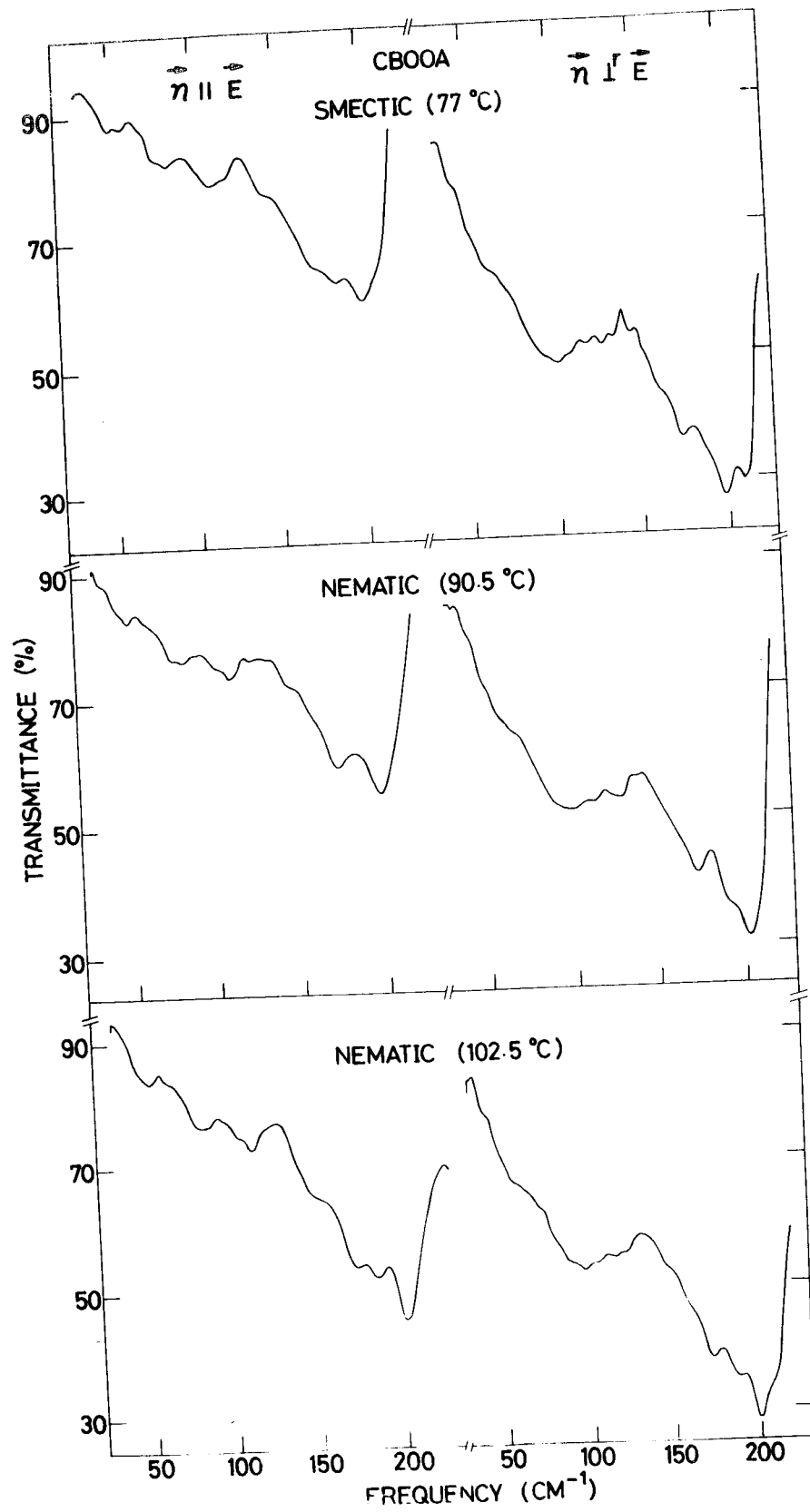
Additional evidence for conformational changes in the octyl tail is discernible from an inspection of Table 4.1 as well as Figure 4.1. Several other spectral features associated with the rocking, twisting and wagging progression modes of the  $(\text{CH}_2)_7$  group as well as the aliphatic C-H stretching frequencies show interesting differences between the two phases. This would be as expected<sup>24</sup> if as compared to the solid, new conformations of the octyl tail are allowed in the smectic phase. The present results thus indicate that the crystal-smectic A transition in CBOOA is accompanied by intramolecular changes associated with the octyl tail and that such changes may be a general feature of solid-mesophase transitions, especially when

the constituent molecules of the mesogen possess long, flexible end chains.

(ii) Dichroic Effects: We now turn to a discussion of the dichroic behaviour of the far-infrared absorption of liquid crystalline CBOOA. To our knowledge, no polarization studies on liquid crystals have been reported so far in the far-infrared region. Figure 4.5 shows the dichroic behaviour of homogeneously aligned samples in the range  $30\text{--}250\text{ cm}^{-1}$ . As noted earlier, the alignment was not quite uniform over the *entire* sample in the nematic phase and it deteriorated noticeably in the smectic A phase. In spite of this departure from uniform alignment, the spectra do show evidence of a clear dichroic behaviour in both smectic A and nematic phases. At frequencies below  $130\text{ cm}^{-1}$ , for incident radiation polarized perpendicular to the direction of alignment, ( $\hat{n} \perp \vec{E}$ ), one observes a strong, broad absorption band centred at  $\sim 100\text{ cm}^{-1}$  in addition to a shoulder at  $\sim 65\text{ cm}^{-1}$ . In contrast, for radiation polarized parallel to the direction of alignment, ( $\hat{n} \parallel \vec{E}$ ), three weak absorption maxima are present at 50, 80 and  $110\text{ cm}^{-1}$ . It should be noted that without the aid of polarization studies, it would have been very difficult to establish the presence of these weak features, as the spectrum is otherwise dominated by the strong band centred at  $\sim 100\text{ cm}^{-1}$ . The modes at  $175$  and  $200\text{ cm}^{-1}$  persist in

**FIGURE 4.5**

Dichroic behaviour of the far-infrared absorption of CBOOA in the smectic A and nematic phases. The sample was homogeneously aligned. The two traces at each temperature correspond to the electric vector being parallel ( $\hat{\mathbf{n}} \parallel \mathbf{E}$ ) and perpendicular ( $\hat{\mathbf{n}} \perp \vec{\mathbf{E}}$ ) to the direction of alignment.



both polarizations, although they are more intense for  $\hat{n} \perp \vec{E}$ .

The spectra do not show any significant changes between smectic A and nematic phases or as a function of temperature. The spectrum in the isotropic phase was essentially a superposition of the spectra shown here for the two different polarizations. This shows that the long range molecular ordering in the liquid crystalline phases has very little effect on the far-infrared absorption of CBOOA. Rather, the spectra appear to be more sensitive to the molecular structure and short range effects in the fluid phases. The broad absorption band at  $100 \text{ cm}^{-1}$  is similar to those observed earlier in other liquid crystals,<sup>3, 9-11</sup> and organic liquids<sup>25</sup>. The weak, yet distinct low frequency structure seen here for  $\hat{n} \parallel \vec{E}$  was not reported in previous studies. Earlier far-infrared studies on liquid crystals were limited to those with relatively shorter molecular end groups, whereas CBOOA possesses a long octyl tail. This suggests that some of the weak modes observed here may be characteristic of the octyl tail. In the case of n-alkanes, normal mode calculations by Schachtschneider and Snyder<sup>26</sup> indicate that such low frequency modes can arise from  $\angle\text{C-C-C}$  bend and  $\text{CH}_2\text{CH}_2$  torsional modes when the polymethylene chain is sufficiently long. Moreover, although p-azoxyanisole itself does not exhibit such modes, a preliminary study



on higher members of its homologous series with hexyl and heptyl end chains indicates<sup>27</sup> that they too possess similar weak bands in this range. These considerations lend additional support to our assignment of these weak bands in CBOOA as originating from the octyl tail.

#### 4.4. Conclusions

The far-infrared spectra of crystalline CBOOA give evidence of pretransition effects as well as intramolecular changes near the crystal-smectic A transition. In the fluid phases, the far-infrared absorption appears to be sensitive to the structure of the molecular end chain. In the case of poly mesomorphic materials, this offers the possibility of investigating the influence of different types of molecular ordering on flexible end chains and the conformational changes associated with them in each phase.

## References

1. W. Maier and G. Englert, Z. Physik. Chem. (NF) 19, 168 (1959).
2. N.M. Amer and Y.R. Shen, J. Chem. Phys. 56, 2654 (1972).
3. E. Sciesinska, J. Sciesinski, J. Twardowski and J.A. Janik, Mol. Cryst. Liquid Cryst. 27, 125 (1974).
4. B.J. Bulkin, G. Grunbaum and A.V. Santoro, J. Chem. Phys. 51, 1602 (1969).
5. S. Kirov and P. Simova, Mol. Cryst. Liquid Cryst. 30, 59 (1975).
6. T. Riste and R. Pynn, Solid State Commun. 12, 409 (1973).
7. R. Pynn, J. Phys. Chem. Solids, 34, 735 (1973).
8. K.K. Kobayashi, Phys. Lett. 31A, 125 (1970); Mol. Cryst. Liquid Cryst. 13, 137 (1971).
9. S. Venugopalan, Pramana Suppl. 1, p. 167 (1975).
10. B.J. Bulkin and W.B. Lok, J. Phys. Chem. 77, 326 (1973).
11. A.S. L'Vova, L.M. Sabirov, I.M. Arefev and M.M. Sushchinskii, Opt. Spectrosc. 24, 322 (1968).
12. J.M. Janik, J.A. Janik and W. Witko, Acta Phys. Polon. A44, 483 (1973).
13. N.M. Amer, Y.R. Shen and H. Rosen, Phys. Rev. Lett. 27, 379 (1971).
14. W.J. Boren, S.S. Mitra and C.W. Brown, Phys. Rev. Lett. 27, 379 (1971).

15. M.J. Billard, M. Delhaye, J.C. Merlin and G.Vergoten, C.R.Acad.Sci.(Paris) B273, 1105 (1971).
16. B.J. Bulkin and F.T. Prochaska, J.Chem.Phys. 54, 635 (1971).
17. W.R. Krigbaum and P.G. Barber, Acta Crystallogr. B27, 1884 (1971).
18. J. Doucet, A.M. Levulet and M.Lambert, Mol.Cryst. Liquid Cryst. 24, 317 (1973).
19. N.M. Amer and Y.R. Shen, Solid State Commun., 12, 263 (1973).
20. D. Drorjetski, V.Volterra and E. Wiener-Avneer, Phys. Rev. A12, 681 (1975).
21. R.F.Schaufele, J.Chem.Phys. 49, 4168 (1968).
22. J.M.Schnur, Mol.Cryst.Liquid Cryst. 23, 155 (1973).
23. H.Takeuchi, T.Shimanouchi, M.Tasumi, G.Vergoten and G. Fleury, Chem.Phys.Letts. 28, 449 (1974).
24. R.G. Snyder, J.Chem.Phys. 47, 1316 (1967).
25. S.R. Jain and S. Walkei, J.Phys.Chem. 75, 2942 (1971).
26. J.H. Schachtschneider and R.G. Snyder, Spectrochim. Acta 19, 117 (1963).
27. S. Venugopalan (unpublished).

Table 4.1

Infrared absorption frequencies (in  $\text{cm}^{-1}$ ) of CBOOA in the solid (Phase I) and smectic A phases, in the range  $30\text{--}3100\text{ cm}^{-1}$  and their proposed assignments.\* The absorption frequencies of solid (Phase I) below  $220\text{ cm}^{-1}$  are also listed here for comparison. Wavelengths corresponding to frequencies above  $730\text{ cm}^{-1}$  are accurate to  $\pm 0.01\ \mu$ ; below  $700\text{ cm}^{-1}$  the frequencies are accurate to  $\pm 2\text{ cm}^{-1}$ .

Solid (Phase I)	Smectic A	Proposed assignment
45 (vw)	50	} $\tau(\text{CH}_2\text{CH}_2)$
70 (sh)	65 (sh)	
84 (sh)	80	
88		
93 (sh)		} $\angle\text{C-C-C bend (C}_8\text{H}_{17})$
98		
101	100	
	110	} Libration $\text{C}_6\text{H}_4$
128	130 (sh)	
157		} $\tau(\text{CH}_2\text{CH}_2)$
166		
	174	} $\tau(\text{CH}_3)$
187		
204	200	
219 (sh)		
274	278	} $\angle\text{C-C-C bend (C}_8\text{H}_{17})$
294		
336 (vw)	334	

↑  
Lattices modes (solid)  
↓

Solid (Phase I)	Smectic A	Proposed assignment	
361 (vw)	361 (vw)	Libration CHN	
389	386		
406			
423	420	$\left. \begin{array}{l} \text{C}_6\text{H}_4\text{-C}\equiv\text{N interaction} \\ \Gamma \end{array} \right\}$	
454	457		
462 (sh)	466		
470 (sh)	474		$\left. \begin{array}{l} \text{C-C-C bend} \\ (\text{C}_8\text{H}_{17}) \end{array} \right\}$
484	482		
499	499		
518			
532	536		
563	559		
592 (sh)	594		
602	602		
638	637	$\left. \begin{array}{l} \Gamma \end{array} \right\}$	
647	646		
662	662		
671	671		
	712 (sh)		
721	720 (sh)	$\left. \begin{array}{l} \text{P}(\text{CH}_2) \end{array} \right\}$	
	728		
754	771	$\begin{array}{c} \uparrow \\ \text{P}(\text{CH}_2) \\ \downarrow \end{array}$	
792	795		$\omega$
809	802 (sh)		

Solid (Phase I)	Smectic A	Proposed assignment
830	825 (sh)	} $\gamma$
840	838	
848 (sh)		
886	884	$\rho(\text{CH}_3)$
	912 (vw)	
927		
933	931	$\rho(\text{CH}_2)$
956	947	} $\gamma$
973	970	
1000	999 (sh)	} $\delta$
1015 (sh)	1018	
1028	1029 (ash)	
1043		
1062 (ah)	1063 (sh)	
1075 (sh)		
1104 (sh)	1103	
1109		
1127	1126 (sh)	$\tau(\text{CH}_2)$
1166	1161	$\omega_c$
	1172 (sh)	
1191	1192	
1217 (sh)		$\gamma(\text{CH}_2)$
1244	1247	C-O-C stretch } $\omega$
1261 (sh)		

Solid (Phase I)	Smectic A	Proposed assignment	
1292	1285	$\tau(\text{CH}_2)$ ↓	
1305 (vw)	1305 (sh)		
1315			
1340 (vw)		$\gamma(\text{CH}_2)$ ↓	
1369	1365		
	1380 (sh)		$\delta(\text{CH}_3)$
1391	1391		
1412	1411		
1459 (sh)	1463 (sh)	$\delta(\text{CH}_2)$ ;	
1470	1472	$\delta(\text{CH}_3)$	
1500	1507	$\omega$ ; $\delta(\text{CH}_3)$	
	1524 (sh)		
1558 (vw)	1561 (sh)		
1575	1578 (sh)		
1589	1591	aa; C=N stretch	
1620	1624		
	1885 (vw)		
	1938 (vw)		
2028 (vw)	2018 (vw)		
2077 (vw)			
2212	2233	C≡N stretch	
	2460 (vw)		
	2527 (vw)		
	2746 (vw)		

Solid (Phase I)	Smectic A	Proposed assignment
2827	2849	C-H stretch ( $C_8H_{17}$ )
2891	2919	
3025 (vw)	3036	C-H stretch ( $C_6H_4$ )

\*Note: sh = shoulder; vw = very weak.

In the case of the symbols describing the proposed assignments, we follow here the notations given in Table 3.3.